A closed-loop model for the coordination of gaze control and decision-making

Demetrio Ferro (demetrio.ferro@upf.edu)
Center for Brain and Cognition, Department of Information and Communication Technologies,
Universitat Pompeu Fabra, 08002, Barcelona, Spain

Tianming Yang (tyang@ion.ac.cn)
Institute of Neuroscience, Key Laboratory of Brain Cognition and Brain-inspired Intelligence Technology,
Center for Excellence in Brain Science and Intelligence Technology, Chinese Academy of Sciences, Shanghai 200031, China

Rubén Moreno-Bote (ruben.moreno@upf.edu)
Center for Brain and Cognition, Department of Information and Communication Technologies,
Universitat Pompeu Fabra, 08002, Barcelona, Spain

Abstract

The study of neural circuitry in visually-guided decision-making has generated extensive research and theoretical models of decision formation. However, the role of gaze in enhancing focal sampling and facilitating shifts to sample alternatives remains unclear. We propose a closed-loop model that integrates decision formation with gaze signals to enhance the sampling of visual options. Visual input is first projected to decision populations, implementing competition via mutual inhibition. The output from these populations drives gaze populations, generating visual shifts that feedback into the decision process. We present simulations based on a two-alternative bundle task, showing that gaze and decision outputs align with behavioral performance in terms of decision accuracy and gaze shift occurrences. The model can be extended to study the role of gaze in decision-making both at behavioral and at neural levels, to test predictions such as whether fewer gaze shifts correlate with shorter reaction times, or if gaze shifts coincide with changes in neural value encoding. Additionally, the model can be applied to explore whether gaze and decision align in sequential alternative presentations or when distractors are present.

Keywords: Decision-making, Gaze-centered decisions, Prefrontal cortex, neural network models, neural encoding of value

Introduction

Decision-making is a fundamental cognitive process involving the integration of distributed information (Kristan, 2008) at multiple levels (Cisek, 2012). Choice formation requires the temporal integration of sensory evidence (Lin, Nie, Zhang, Chen, & Yang, 2020) compared via mutual inhibition in neural circuits (Levine & Leven, 1991; Wang, 2008; Koyama & Pujala, 2018; Ballesta & Padoa-Schioppa, 2019; Roach, Churchland, & Engel, 2023), primarily located in frontal brain regions (Rushworth, Noonan, Boorman, Walton, & Behrens, 2011).

In visually-guided decisions, gaze enhances focal vision by highlighting relevant information (Deubel & Schneider, 1996; Shadlen, Kiani, Hanks, & Churchland, 2008; Hajnal et al., 2024), enhancing the encoding of the value of visually sampled options, and of choices performed via saccadic responses (McGinty, Rangel, & Newsome, 2016; Smith & Krajbich, 2019; Ferro, Cash-Padgett, Wang, Hayden, & Moreno-Bote, 2024). Previous theoretical work on gaze-centered decision-making mainly focused on the feed-forward interaction between gaze position and value (Krajbich, Armel, & Rangel, 2010; Hare, Schultz, Camerer, O'Doherty, & Rangel, 2011), using approaches based on stochastic drift diffusion of decision signals (Usher & McClelland, 2001).

We propose a closed-loop model where decision formation, driven by mutual inhibition between two choice-selective populations, influences neural populations generating gaze signals modeled via bistable network dynamics (Moreno-Bote, Rinzel, & Rubin, 2007). Gaze alternation modulates the feedback to decision-forming populations. Inspired by a two-alternative visual bundle task (Huang et al., 2024), this framework allows the comparison of theoretical insights with empirical data to investigate the role of gaze in decision-making.

Methods

The two-alternative bundles decision-making task. The two-alternative bundles task (Huang et al., 2024) consists of the simultaneous presentation of two bundles of visual items. Each bundle contains 3 shape items disposed vertically either on the left or on the right of the screen ($s_{k,L}$, or $s_{k,R}, k = 1,2,3$). The respective items are associated to rewards whose nominal value ranges between 0 and 5. The value of the two bundles ($bv_L = \sum_{k=1}^{3} s_{k,L}, bv_R = \sum_{k=1}^{3} s_{k,R}$) ranges between 0 and 15. The subjects report their decision by directing their gaze to the chosen bundle, and holding fixation on it for 400 ms. Correct choice consists in selecting the bundle with highest value, rewarded with liquid of size proportional to best bundle value. Incorrect choices incur in a 3 s time time-out penalty.

The gaze and decision model. The interaction between decision formation and gaze direction is modeled by hypothesizing mutual inhibition between the respective (1, decision; 2, gaze) population pairs (each containing L, left or R, right units). We supposed that the bundle shapes ($s_{k,L}, s_{k,R}, k = 1,2,3$) are visually sampled by multiplication to gaze bias signals ($b_L(t), b_R(t)$). The left or right bundle sampling is fed to the respective decision populations through scaling factors $\alpha_L^{(1)}, \alpha_R^{(1)}$, implementing choice formation. The output of deci-

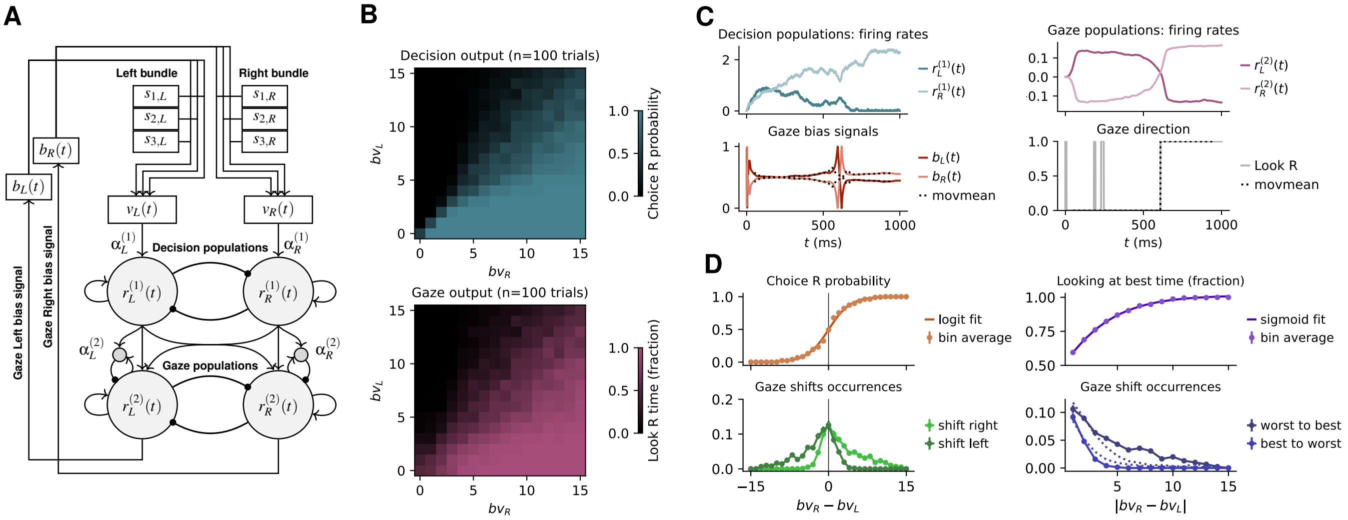

Figure 1: **Model diagram and simulation results. A.** Model diagram outline. **B.** Probability of choosing the right option (top) and fraction of time directing gaze to right bundle side (bottom) for all pairs of right and left bundle values (bv_R, x-axis, bv_L, y-axis). Parameters used: $dt = 0.1$ ms, $\tau^{(1)} = 100$ ms, $\tau^{(2)} = 30$ ms, $w_{LL}^{(1)} = w_{RR}^{(1)} = 0.05$, $w_{LR}^{(1)} = w_{RL}^{(1)} = -1$, $w_{LL}^{(2)} = w_{RR}^{(2)} = 0.5$, $w_{LR}^{(2)} = w_{RL}^{(2)} = -2$, $\alpha^{(1)} = 1, \alpha^{(2)} = 0.1$, $\sigma_{(1)} = 5, \sigma_{(2)} = 0.08, \tau_\xi = 1000$ ms, $b_0 = 0, b_1 = 1$. **C.** Firing rate of the neural populations (decision, top left; gaze, top right) and gaze signals (bias, bottom left; direction, bottom right) for a sample trial configuration ($bv_L = 4, bv_R = 5$). Gaze signals panels include moving mean filtered versions (dotted, movmean). **D.** Task psychometrics for bundle value differences: probability of right bundle choice and logistic fit (top left), fraction of time looking at best option and sigmoidal function fit (top right), average occurrence of gaze shifts between the two bundles sides (bottom left) and of gaze shifts towards best/worst option (bottom right), with dotted lines showing comparison with gaze shifts from empirical experiments by Huang et al. (2024).

sion populations is combined before being projected through scaling factors to gaze populations implementing attractor networks with perceptual bistability, allowing alternations induced by noise fluctuations (Moreno-Bote et al., 2007). The gaze bias signals $b_L(t), b_R(t)$ are fed back to model visual sampling.

The firing rates of the two (L/R) population pairs $(r_L^{(i)}(t), r_R^{(i)}(t), i = 1,2)$ are modeled by the following equations:

$$\begin{aligned}\tau_L^{(i)}\frac{dr_L^{(i)}}{dt} &= -r_L^{(i)}(t) + f\left(w_{RL}^{(i)} r_R^{(i)}(t) + w_{LL}^{(i)} r_L^{(i)}(t) + I_L^{(i)}(t) + \xi_L^{(i)}(t)\right)\\ \tau_R^{(i)}\frac{dr_R^{(i)}}{dt} &= -r_R^{(i)}(t) + f\left(w_{LR}^{(i)} r_L^{(i)}(t) + w_{RR}^{(i)} r_R^{(i)}(t) + I_R^{(i)}(t) + \xi_R^{(i)}(t)\right)\end{aligned} \tag{1}$$

$$\begin{matrix} v_L(t) = b_L(t)\sum_{k=1}^{3} s_{k,L} \\ v_R(t) = b_R(t)\sum_{k=1}^{3} s_{k,R} \end{matrix}, \quad \begin{matrix} I_L^{(1)}(t) = \alpha_L^{(1)} v_L(t) \\ I_R^{(1)}(t) = \alpha_R^{(1)} v_R(t) \end{matrix}, \tag{2}$$

$$\begin{matrix} g_L(t) = \alpha_L^{(2)} r_L^{(1)}(t) \\ g_R(t) = \alpha_R^{(2)} r_R^{(1)}(t) \end{matrix}, \quad \begin{matrix} I_L^{(2)}(t) = g_L(t) - (g_L(t) + g_R(t))\, r_L^{(2)}(t) \\ I_R^{(2)}(t) = g_R(t) - (g_R(t) + g_L(t))\, r_R^{(2)}(t) \end{matrix}. \tag{3}$$

The terms $\xi_L^{(1)}(t), \xi_R^{(1)}(t) \sim \mathcal{N}(0, \sigma_{(1)}^2)$, while $\xi_L^{(2)}(t), \xi_R^{(2)}(t)$ are Ornstein-Uhlenbeck processes, with stochastic equations

$$\frac{d\xi}{dt} = -\frac{\xi(t)}{\tau_\xi} + \sigma_{(2)}^2\sqrt{2/\tau_\xi}\, z(t), \;\; z(t) \sim \mathcal{N}\left(0, \sigma_{(2)}^2\right), \tag{4}$$

and steady-state distribution $\sim \mathcal{N}(0, \sigma_{(2)}^2/(2\tau_\xi))$. We used ReLU for decision populations, modeling thresholded accumulation, and tanh for gaze populations, following general practice respectively from evidence accumulation and bistable switching neural dynamic models. We define feedback gaze bias as

$$b_L(t) = b_0 + b_1\frac{|r_L^{(2)}(t)|}{|r_L^{(2)}(t)| + |r_R^{(2)}(t)|}, \;\; b_R(t) = b_0 + b_1\frac{|r_R^{(2)}(t)|}{|r_L^{(2)}(t)| + |r_R^{(2)}(t)|}. \tag{5}$$

Decision output is sampled at $T = 1000$ ms: choose R if $r_R^{(1)}(T) > r_L^{(1)}(T)$, at $T = 1000$ ms, choose L otherwise. This setting allows capturing full dynamics, though it does not preclude making more detailed assumptions about choice deliberation that may occur earlier, eventually indicated via gaze fixation. We apply a moving mean filter (movmean) on gaze bias signals using boxcar time windows with duration 100 ms and shifted at each 10 ms time offsets. The gaze direction output is determined as: Look R if movmean($b_R(t)$) >movmean($b_L(t)$), Look L otherwise.

Choice probability and looking times. The average fraction of choices for the right side bundle (Fig. 1D, top left) is computed in discrete bins of bundle value difference, and overlaid to the logistic fit of trial-based data, modeling choice probability as $P(ch = R) = 1/(1 + e^{-\beta_0 - \beta_1(bv_R - bv_L)})$.

Gaze direction and shifts. We computed the average fraction of time looking at best bundle (Fig. 1D, top right) in binned values of absolute bundle value difference. Trial-based data are fit to $F_{best} = a_0 + a_1/(1 + e^{-\beta_0' - \beta_1'|bv_R - bv_L|})$. Gaze shifts are defined as temporal discontinuities in Look L / Look R, computed in 10 ms bins via discrete-time differentiation.

Results.

We computed the fraction of choices for right bundle and the fraction of time spent directing the gaze to right bundle, generating 100 trials for each (bv_L, bv_R) pair (Fig. 1B). We show the firing rates in a sample configuration (Fig. 1C). The decision is significantly related with bundle values (Fig. 1D top left, $\beta_0 = -0.01, \beta_1 = 0.48, p < 0.001$). The generated gaze signals are directed for most part of the time towards the bundle with the best value (Fig. 1D top right, $a_0 = -0.1, a_1 = 1.11, \beta'_0 = 0.14, \beta'_1 = 0.35$). Gaze shifts most often occur at low bundle value differences (Fig. 1D, bottom), more frequently directed to right/left bundle when right/left bundle has the best value (Fig. 1D, bottom left). This is also shown by combining best/worst shifts at absolute value difference bins (Fig. 1D, bottom right). All results qualitatively align with behavioral patterns reported by Huang et al. (2024), though empirical overlays are shown only for gaze shifts (Fig. 1D, bottom right, dotted lines) due to partial data availability. At the current stage, other panels could only be qualitatively compared against the same dataset. Beyond shown results, the model supports testable predictions about gaze–choice interactions, e.g., whether fewer gaze shifts lead to shorter reaction times, or if gaze shifts coincide with neural encoding alternations, while capturing known bidirectional effects such as post-decisional gaze bias. Though not directly compared to drift-diffusion models, our circuit-level approach captures dynamic feedback unavailable to feedforward DDMs. Additionally, the model can be extended to explore gaze–decision dynamics across more complex paradigms and may relate to neural systems such as LIP or FEF involved in oculomotor planning and value encoding.

Acknowledgments

This work was supported by the Ministry of Science, Innovation and Universities (MICIU/AEI/10.13039/501100011033, Spain), “FEDER: A way of making Europe” (ref: PID2023-146524NB), ICREA ACADÈMIA (2022).

References

Ballesta, S., & Padoa-Schioppa, C. (2019). Economic decisions through circuit inhibition. *Current Biology*, *29*(22), 3814–3824.

Cisek, P. (2012). Making decisions through a distributed consensus. *Current opinion in neurobiology*, *22*(6), 927–936.

Deubel, H., & Schneider, W. X. (1996). Saccade target selection and object recognition: Evidence for a common attentional mechanism. *Vision research*, *36*(12), 1827–1837.

Ferro, D., Cash-Padgett, T., Wang, M. Z., Hayden, B. Y., & Moreno-Bote, R. (2024). Gaze-centered gating, reactivation, and reevaluation of economic value in orbitofrontal cortex. *Nature Communications*, *15*(1), 6163.

Hajnal, M. A., Tran, D., Szabó, Z., Albert, A., Safaryan, K., Einstein, M., ... Orbán, G. (2024). Shifts in attention drive context-dependent subspace encoding in anterior cingulate cortex in mice during decision making. *Nature communications*, *15*(1), 5559.

Hare, T. A., Schultz, W., Camerer, C. F., O’Doherty, J. P., & Rangel, A. (2011). Transformation of stimulus value signals into motor commands during simple choice. *Proceedings of the National Academy of Sciences*, *108*(44), 18120–18125.

Huang, Y., Zhu, R., Sun, R., Zhang, W., Ren, C., Zhao, Z., & Yang, T. (2024). Value computation of offer bundles in prefrontal circuits during economic decision-making. In *The 17th annual meeting of chinese neuroscience society.*

Koyama, M., & Pujala, A. (2018). Mutual inhibition of lateral inhibition: a network motif for an elementary computation in the brain. *Current opinion in neurobiology*, *49*, 69–74.

Krajbich, I., Armel, C., & Rangel, A. (2010). Visual fixations and the computation and comparison of value in simple choice. *Nature neuroscience*, *13*(10), 1292–1298.

Kristan, W. B. (2008). Neuronal decision-making circuits. *Current Biology*, *18*(19), R928–R932.

Levine, D. S., & Leven, S. J. (1991). Inhibition in the nervous system: Models of its roles in choice and context determination. *Neurochemical research*, *16*, 381–395.

Lin, Z., Nie, C., Zhang, Y., Chen, Y., & Yang, T. (2020). Evidence accumulation for value computation in the prefrontal cortex during decision making. *Proceedings of the National Academy of Sciences*, *117*(48), 30728–30737.

McGinty, V. B., Rangel, A., & Newsome, W. T. (2016). Orbitofrontal cortex value signals depend on fixation location during free viewing. *Neuron*, *90*(6), 1299–1311.

Moreno-Bote, R., Rinzel, J., & Rubin, N. (2007). Noise-induced alternations in an attractor network model of perceptual bistability. *Journal of neurophysiology*, *98*(3), 1125–1139.

Roach, J. P., Churchland, A. K., & Engel, T. A. (2023). Choice selective inhibition drives stability and competition in decision circuits. *Nature communications*, *14*(1), 147.

Rushworth, M. F., Noonan, M. P., Boorman, E. D., Walton, M. E., & Behrens, T. E. (2011). Frontal cortex and reward-guided learning and decision-making. *Neuron*, *70*(6), 1054–1069.

Shadlen, M. N., Kiani, R., Hanks, T. D., & Churchland, A. K. (2008). An intentional framework. In *Neurobiology of decision making* (chap. 4). MIT Press Direct.

Smith, S. M., & Krajbich, I. (2019). Gaze amplifies value in decision making. *Psychological science*, *30*(1), 116–128.

Usher, M., & McClelland, J. L. (2001). The time course of perceptual choice: the leaky, competing accumulator model. *Psychological review*, *108*(3), 550.

Wang, X.-J. (2008). Decision making in recurrent neuronal circuits. *Neuron*, *60*(2), 215–234.